
Maurizio Sansotera


Walter Navarrini

FEDERICO PERSICO[1,2], MAURIZIO SANSOTERA[1,2*], NICOLE SCHEPIS[1], LUCA MAGAGNIN[1], WALTER NAVARRINI[1,2*]

* Corresponding authors

1. Dipartimento di Chimica, Materiali e Ingegneria Chimica "Giulio Natta", Politecnico di Milano, Via Mancinelli 7, 20131, Milano, Italy

2. Consorzio Interuniversitario Nazionale per la Scienza e Tecnologia dei Materiali, Via G. Giusti 9, 50121 Firenze, Italy

Synergic photocatalytic effect between TiO_2 and a fluorinated transparent ionomeric material in the oxidation of hydrosoluble pollutants in turbid suspensions

KEYWORDS: Photocatalysis; water treatment; turbid solution; titanium dioxide; Crystal Violet; advanced oxidation processes.

Abstract

The crystal violet (CV) dye has been chosen to study the photooxidation activity of titanium dioxide immobilized into a transparent fluoropolymeric matrix toward organic pollutants. The photoactive matrix was directly coated on the UV source by applying a TiO_2 containing fluorinated ionomeric dispersion and a perfluorinated transparent amorphous polymer in an appropriate sequence. The photocatalytic activity of the multilayered coating towards the hydrosoluble organic CV dye was evaluated in transparent solution and in highly turbid suspension. The turbidity was obtained by dispersing insoluble microparticles of calcium sulfate in the polluted aqueous solution. The photoabatement rates obtained in transparent and in turbid conditions were 0.0918 min^{-1} and 0.0300 min^{-1}, respectively. The TiO_2 nanoparticle dispersed in the fluorinated matrix revealed a higher photocatalytic activity than simple dispersed TiO_2 in both transparent as well as turbid conditions. The immobilization of the catalyst in a stable fluorinated matrix avoided the TiO_2 separation and prevented catalyst losses. The synergism in the activity between the TiO_2-based photocatalyst and the fluorinated matrix was particularly evident at low pollutant concentrations.

INTRODUCTION

Advanced oxidation processes (AOPs) have been widely recognized as performing alternatives to conventional methods for removal of organic pollutants from water and wastewater (1-3). In particular, semiconducting transition metal oxides revealed remarkable catalytic properties in the presence of UV light, suggesting new promising applications in the field of photocatalysis (4-6). Anatase titanium dioxide, TiO_2, has a band gap of 3.2 eV and pairs of holes (h^+) and electrons (e^-) are efficiently formed when its surface is exposed to radiations with wavelengths below 385-410 nm. Electron-hole pairs can either recombine or react with adsorbed electron donor or acceptor molecules (7). In the presence of water and oxygen, hydroxyl radicals OH· and superoxide ions O_2^{-}· can be generated (7). These radicalic intermediates are strong oxidizing species able to oxidize organic compounds (8, 9). Direct oxidation at the hole site is usually favored in case of highly adsorbed substrates, while the degradation of weakly adsorbed pollutants takes place mainly through hydroxyl radical mediated oxidation (10,11). Therefore, the oxidation of organic pollutants can be described either with a direct oxidation with the photogenerated holes, or with a hydroxyl radicals mediated oxidation as well as a combination of the two (12, 13).
The use of photocatalytic TiO_2 nanoparticle in suspension or slurry-type reactors has been reported to be well-performing, especially because of the high surface area of the catalyst available for the process (14-16). However, the industrial feasibility of such systems is limited due to the low quantum efficiency for slurry processes and because of the necessity of a costly post-treatment for catalyst recovery by solid-liquid separation (5, 7, 10, 13).
This work is focused on the development of a perfluorinated multilayered transparent coating with embedded TiO_2 particles, able to promote photocatalytic degradation of hydrosoluble organic pollutants in both transparent and turbid conditions; this methodology can avoid also the needing of a post-treatment stage for catalyst recovery. The polymeric matrix suitable for this application required several chemical and physical properties, such as chemical stability towards UV-activated TiO_2, stability and transparency towards UV light, high permeability to O_2 and water vapor (both indispensable in photocatalytic oxidations) and high water affinity. The use of perfluoropolymers as coating materials for anodized titanium substrates allows an increase in surface washability, resistance to soiling (12) and gas phase permeability (14, 15). It is well known that soiling on TiO_2 thin layers can easily deactivate the catalyst (16). Perfluoropolymeric materials, due to the presence of highly stable C–F bonds (17), are characterized by high thermal and chemical stability (17, 18), particularly towards UV radiation and UV-activated TiO_2 (19), low surface energy and high transparency for amorphous fluoropolymers (12, 20, 21). The interaction between the dispersed TiO_2 catalyst and the aqueous polluted solution was optimized by the use of a ionomeric copolymer of

tetrafluoroethylene (TFE) and fluorosulfonyl vinyl ether (FSVE) characterized by the presence of sulfonic high acidic groups (22). Perfluorinated ionomeric membranes have a wide range of applications owing to their excellent chemical and thermal stability, ion conductivity and UV transparency (23, 24).The perfluorinated multilayered ionomeric photoactive matrix was directly applied on the quartz sheath of the UV source, allowing also the efficient treatment of turbid solutions. Indeed, the inner interface adherent to the UV source was preserved clean and transparent to UV light, while through the outer interface between the perfluorinated ionomeric coating and the aqueous phase, the pollutants were free to diffuse towards the activated TiO_2 nanoparticles dispersed in the ionomeric phase.

The photocatalytic activity of the hybrid coating was evaluated by studying the degradation of Crystal Violet (CV), a hydrosoluble dye. CV was chosen as a molecular model of persistent organic pollutant with genotoxic and carcinogenic effects on immune and reproductive systems; in particular, its polyaromatic structure makes it barely treatable by conventional method (25-27). Moreover, aqueous solutions of CV show a typical deep violet color due to the strong absorption at 590 nm detectable even at low dye concentrations (up to 10^{-6} M). This peculiarity is not affected by mild pH variations; in strongly acidic conditions (pH ranging from 1 to -1), the hue of the dye solution changes from violet to green, with absorption maxima at 420 and 620 nm, and finally to yellow, with an absorption maximum at 420 nm (28). The different colors are due to different charged states of the CV molecule: only one of the three nitrogen atoms in the molecule is positively charged at neutral pH; the green color corresponds to a form where two nitrogen atoms are positively charged and one of them is protonated; in the yellow-colored form all nitrogen atoms carry a positive charge and two of them are protonated (28). Although the mechanism of photocatalysis has still not been completely clarified, CV mineralization reaction could be ideally summarized as reported in Equation 1:

$$2\,C_{25}H_{30}N_3Cl + (129/2 + 3x)\,O_2 \rightarrow 50\,CO_2 + 27\,H_2O + 2\,H_3O^+ + 6\,NO_x + 2Cl^- \quad \text{(Eq.1)}$$

The photocatalytic degradation of CV in aqueous solution and in the presence of photogenerated radicalic species can start in correspondence to the central carbon of the dye molecule, causing the chromophore cleavage with the formation of 4-(*N*,*N*-dimethylamino)-4'-(*N*',*N*'-dimethylamino) phenone and 4-(*N*,*N*-dimethylamino)phenol, or can proceed via *N*-deethylation. Further degradation occurs through the formation of 4,4'-bis-aminobenzophenone and 4-aminophenol that are in the end mineralized (Scheme 1) (25-27).

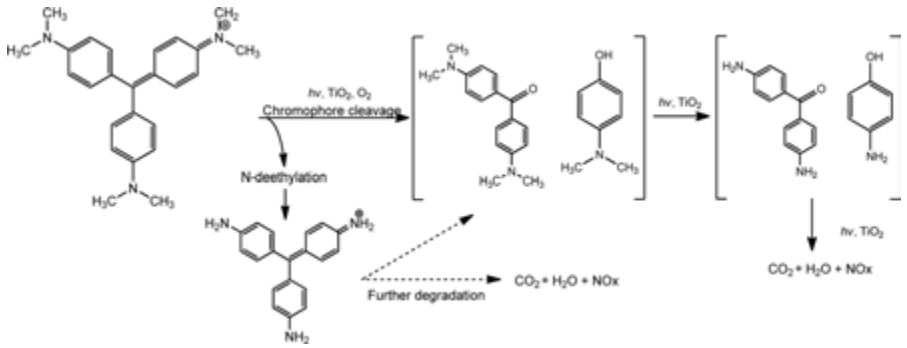

Scheme 1. Photocatalytic degradationof CV induced by TiO_2.

MATERIALS AND METHODS

Materials

Nanometric titanium dioxide P-25 (75% Anatase, 25% Rutile; supplied by Evonik®) in powder was employed as photocatalyst. The photoactive coating applied over the quartz sheath was realized with AQUIVION® D83-06A (AQ) and HYFLON® AD60 (AD), whose molecular structures are reported in Figure 1-a and 1-b, respectively; both fluoropolymers are produced, commercialized and supplied by Solvay Specialty Polymers. AQ, used as received for the experimental tests, is a melt-extruded ionomeric branched copolymer, obtained from TFE and a FSVE of formula F_2C=CF-O-CF_2-CF_2-SO_2F. AQ starting material is in the acidified form, in a 6% solution of 1propanol (40%), 2-propanol (40%) and water (20%), and it has an equivalent weight of 830 g/eq, total acid capacity of 1.17-1.23 meq/g and density of 0.875 g/cm^3. The SO_3H groups are placed as terminals of the lateral chains, conferring hydrophilicity and consequently good wettability to the photoactive coating, whereas the backbone of the polymer is hydrophobic due to the presence of C–F bonds. AD is a random copolymer of TFE and 2,2,4-trifluoro-5-trifluoromethoxy-1,3-dioxole (TTD), characterized by outstanding chemical stability (15), low refractive index (equal to 1.327) and T_g of 130°C (15). AD was employed in solution during the experimental tests, using GALDEN® HT110 (Solvay Specialty Polymers) as solvent. GALDEN® HT110 is a PFPE-based solvent with boiling point of 110°C and formula as follow:
$CF_3O(CF_2CF(CF_3)O)_p(CF_2O)_nCF_3$ (p + n = 2-3; p/n = 20-50).
Crystal Violet (CV), namely tris(4-(dimethylamino)phenyl) methylium chloride, is a triarylmethane dye with formula $C_{25}H_{30}N_3Cl$ (MW = 407.98 g/mol) and water solubility of 16 g/L. $CaSO_4$ micrometric powder (Laviosa Chimica Mineraria S.p.A. - Livorno) is insoluble in water and photochemically inert and it was chosen as white solid to generate turbidity in solution. The average particle size was estimated by SEM analysis and it was found to be in the range between 1 and 20 μm.

Photoactive coating

The preparation of a stable photoactive coating on the quartz sheath (Figure 2) was obtained by employing two different perfluoropolymer in solutions: a 10%$_{wt}$ solution of AD (Fig. 1-b) in Galden® HT110 perfluoropolyether and a 6%$_{wt}$ solution of AQ (Figure 1-a) in a hydroalcoholic solvent (water/*i*-propanol/*n*-propanol 20:40:40) containing 0.6%$_{wt}$ of dispersed active nanometric TiO_2. The former acted as hydrophobic fluorinated primer and the latter as hydrophilic photoactive layer. The first two layers in contact with the UV source consisted in AD polymer: the AD first layer was directly in contact with the quartz sheath surface, acting as

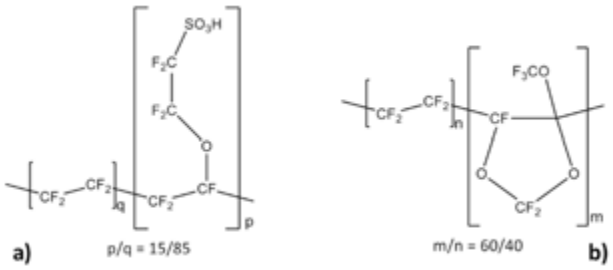

Figure 1. Molecular structures of Aquivion® D83-06A (a), Hyflon® AD60 (b).

effective hydrophobic primer, and it was thermally cured as described in our previous work in order to increase the adhesion and prevent water from penetrating between the coating and the sheath (5). The second AD layer was not thermally treated and it allowed the adhesion between the perfluorinated hydrophobic layer and the ionomeric hydrophilic photoactive layer by entanglement of fluorinated chains and fluorous interactions.
The fine dispersion of TiO_2 (average aggregate dimension = 1 μm) in the hydroalcoholic AQ solution was obtained by ultra-sonication for 30 min at room before its application on the sheath. The AQ layer with embedded TiO_2 was deposited on the surface of AD layers and, subsequently, it was thermally cured with a specific heating program described in our previous work in order to evaporate the solvents and to promote the adhesion between perfluoropolymeric layers (5). AQ, as fluorinated polymer is permeable to aqueous pollutants and, in particular, promotes the direct contact between the activated TiO_2 and CV. Both fluorinated polymeric AD and AQ layers are chemically stable towards the degradation effects due to redox photocatalytic activity of TiO_2 and to UV light under oxygen atmosphere (15).

Experimental apparatus

The reaction apparatus (Figure 2) consisted of a stirred semi-batch 0.5 L glass reactor (diameter: 6.5 cm) realized to contain a low pressure Hg UV lamp (Engelhard Hanovia®, with nominal power absorption of 4 W, emitting light at wavelengths of 240-300 nm with emissivity of 0.2 W/m^2) inserted into a 2 mm thick quartz sheath. The UV lamp was cooled with a flux of nitrogen in order to maintain constant the solution temperature (25 ± 3°C).

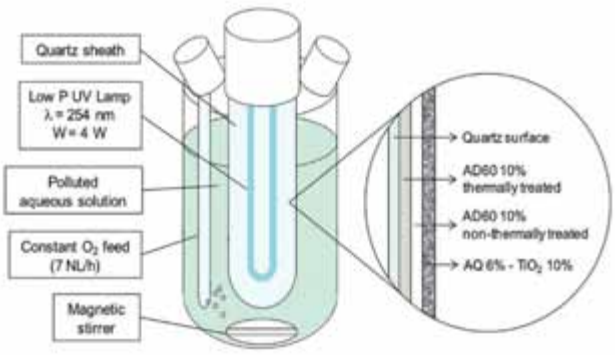

Figure 2. Experimental apparatus and details of the photoactive coating.

The emissivity of the UV lamp was measured with a Delta Ohm HD 2102.2 radiometer in the presence of the coated as well as uncoated quartz sheath. Due to the lamp geometry, the emissivity resulted constant along its cylindrical bulb and significantly decreased at the tip. The photoactive coating caused an evident variation in the lamp emissivity values. In fact, the average light intensities from the sheath surface were (123 ± 7) · 10^{-3} W/m^2 for the uncoated quartz sheath and (57 ± 4) · 10^{-3} W/m^2 after the application of the photoactive coating. The observed decrease in emissivity was higher than about 54% and it was completely ascribable to the UV absorption by TiO_2, because of AQ and AD UV transparency.
Overall, the AQ-based photocatalytic coating resulted adherent to the external surface of the sheath and in direct contact with the aqueous polluted solutions, with a surface/volume ratio of 0.048 m^2/L. The average photon flux (Φ) generated by the low pressure Hg UV lamp was 261 nmol/(m^2·s); in the presence of the photoactive coating, the fraction of photon flux absorbed by dispersed TiO_2 was 140 nmol/(m^2·s), while the remaining radiation reached the polluted aqueous solution. The average light intensity outside the reactor in the presence of dispersed TiO_2 powder particles (slurry) was (68 ± 3) · 10^{-3} W/m^2 and, therefore, the fraction of photon flux absorbed by the catalyst slurry resulted 144 nmol/(m^2·s), in addition has been considered negligible the absorption due to CV in solution (about 2 · 10^{-3} W/m^2). Oxygen is required in the photocatalytic reaction and it was fed at the bottom of the reactor. The oxygen flux was regulated at 7 NL/h in the presence of constant magnetic stirring: these two actions generated enough turbulence into the system to assume a constant concentration of O_2 in solution and into the photoactive coating, along with a homogeneous concentration of CV.

Experimental procedure

Ionomeric materials are able to absorb considerable quantities of water, by increasing their volumes and consequently the average pore dimension; thus, before each experimental test the photoactive coating was hydrated with deionized water for 24 h at room temperature. The CV molar absorption coefficients (ε) were obtained through a linear regression of the averaged values of maximum absorbance at 590 nm of five solutions at known dye concentration (within 1·10^{-6} and 2·10^{-5} M): ε was found equal to 76924 M^{-1}·cm^{-1} (R^2 = 0.9966). Each test was performed by filling the reactor with 0.25 L of CV polluted aqueous solution (1.5·10^{-5} M), obtained by diluting a CV stock solution (1·10^{-3} M). The initial sample was collected at time zero, before feeding the CV solution to the reactor; subsequent samplings were taken after regular time intervals. Each CV sample (2 mL) was analyzed by using an UV-Visible Hewlett-Packard 8452A Diode Array spectrophotometer. Samples were scanned four times, the averaged values of the absorbance peaks at 590 nm were calculated and the trends of the ratio between dye concentration at the generic time (C) and at the time zero (C_0) were evaluated. The apparent kinetic constant values (k_{app}) of CV abatement were calculated by supposing pseudo-first order reaction rates.
The photocatalytic activity of the TiO_2-embedded perfluorinated coating was evaluated by monitoring the CV abatement trends under UV irradiation (**Pc-C** test) as well as in turbid conditions (**Pc-Ct** test). The turbidity was

obtained by adding $CaSO_4$ microparticles (8 g/L, average particle dimension = 4 μm) to CV solution. In the tests with turbidity due to $CaSO_4$, the samples were centrifuged in an Eppendorf MiniSpin (13400 rpm - 4 min) before UV-Vis analyses, in order to remove the dispersed particles. The absorption of CV on $CaSO_4$ particles resulted negligible, as evaluated by the decrease in CV concentration in an aqueous CV/$CaSO_4$ dispersion stirred for 24 h (CV decrease < 2%).
The photocatalytic activity of the coating was compared to the performances of a suspension of TiO_2 powder (slurry) in both standard (**Pc-S** test) and turbid conditions (**Pc-St** test). Tests with TiO_2 slurry was performed by dispersing the same amount of TiO_2 photocatalyst which was contained in the photoactive coating (*i.e.* 8 mg/L). The dye removal in the **Pc-C** photocatalytic test was due to simultaneous different phenomena; thus, appropriate accessory tests were performed in order to evaluate each contribution to CV degradation, as reported in Table 1: photolysis in both standard (**Ph-C** test) and turbid conditions (**Ph-t** test); CV absorption on the photoactive coating in the absence of UV irradiation (**Abs-C** test); CV absorption on TiO_2 powder (**Abs-S** test). In particular, the photolysis was evaluated by depositing on the active coating two additional UV transparent AD layers (barrier coating) which prevented the CV diffusion from the solution into the ionomeric photocatalytic layer.

Fluorine-19 nuclear magnetic resonance (^{19}F-NMR) spectroscopy

^{19}F-NMR experiments were performed on a Bruker 500 Ultrashield spectrometer operating at 470.30 MHz. In particular, samples of the solution collected from the reactor at the end of the photoabatement tests were analyzed by ^{19}F-NMR, using D_2O as a deuterated solvent. The absence of signals ascribable to any water-soluble fluorine-containing compounds in the aqueous solution can confirm the chemical stability of the polymeric layers (AQ and AD) in the perfluorinated photoactive coating.

Test	Description	Catalyst	UV lamp emissivity (W/m^2)	TiO_2 slurry (mg/L)	$CaSO_4$ (g/L)
Pc-C	Photocatalysis	Photoactive coating	0.2	0	0
Pc-Ct	Photocatalysis in turbid conditions[b]	Photoactive coating	0.2	0	8[c]
Pc-S	Photocatalysis in slurry	TiO_2 powder	0.2	8	0
Pc-St	Photocatalysis in slurry and turbid conditions[b]	TiO_2 powder	0.2	8	8[c]
Ph-C	Photolysis (*Barrier coating*)	-	0.2	0	0
Ph-t	Photolysis in turbid conditions[b]	-	0.2	0	8[c]
Abs-C	Absorption	Photoactive coating	0	0	0
Abs-S	Absorption in slurry	TiO_2 powder	0	8	0

a. $[CV]_0 = 1.5 \cdot 10^{-5}$ M; T = 25 ± 3°C; constant stirring; O_2 feed = 7NL/h.
b. Turbid conditions were obtained by dispersing $CaSO_4$ powder in the aqueous CV solution.

Table 1. Experimental conditions of CV kinetic testsa.

RESULTS AND DISCUSSION

Perfluorinated ionomers exhibit high ion-exchange capacities in water; in these conditions, hydrophilic continuous water phases inside the hydrophobic fluorinated matrix are formed (23, 29). This multi-phase matrix is characterized by strongly acid sulfonic moieties and it is responsible for the superior ion conductivity typical of the fluorinated membranes.
The presence of the acidic sulfonic side chain terminals promoted the basic pollutant phasetransfer from the aqueous solution-polymer interface into the water phases within the ionomeric matrix. Thus, the acidic nature of the ionomeric photoactive layer promoted an increase in the CV concentration localized in the immediate vicinity of the immobilized TiO_2; in the presence of UV light and oxygen, pollutants were degraded by photoactivated TiO_2 particles, generating mineralization products which retro-diffused to the aqueous phase. The UV-promoted TiO_2 activation and the CV diffusion occurred respectively at two opposite sides of the photoactive coating. Through the outer side the CV molecules (ions) diffused from the aqueous phase to the TiO_2 in the ionomeric phase; on the inner side the perfluorinated layers adherent to the UV source were preserved clean and transparent to UV-light, preventing the scattering due to external contaminants.
The chemical stability of both AD and AQ towards the degradative effects of photoactivated TiO_2 were confirmed by ^{19}F-NMR analysis that revealed the absence of signals ascribable to fluoride release in the aqueous solution during CV photoabatement.

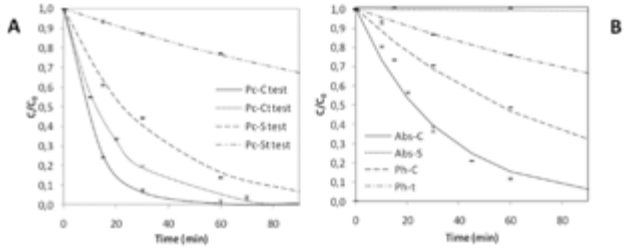

Figure 3. CV photodegradation kinetic curves (A) obtained by using the photoactive coating (**Pc-C** test), the photoactive coating in turbid conditions (**Pc-Ct** test), TiO_2 slurry (**Pc-S** test), TiO_2 slurry in turbid conditions (**Pc-St** test); absorption tests (B) on photoactive coating (**Abs-C** test) and on TiO_2 slurry (**Abs-S** test) as well as photolytic tests (B) in the presence of the photoactive coating with a barrier coating (**Ph-C** test) and in turbid conditions (**Ph-t** test).

In Figure 3 a comparison of the kinetic curves obtained from the main photocatalytic tests of CV abatement has been reported. The photoactive coating (**Pc-C**, **Pc-Ct** tests) achieved definitely higher CV abatement rates than TiO_2 powder as a slurry (**Pc-S** test). This result can be explained by considering the basic nature of CV. Thus, it is worth noticing a synergic effect between the acid/base reactions promoted by the ionomeric superacidic material and the photodegradation properties of TiO_2 photocatalyst. In particular, this synergism is significantly evident at very low pollutant concentration where the photoactive coating is very active if compared to the standard TiO_2 slurry (Figure 3).

Degradation reactions appeared to follow pseudo-first order kinetics (correlation coefficient $R^2 > 0.99$ - Figure 4) which

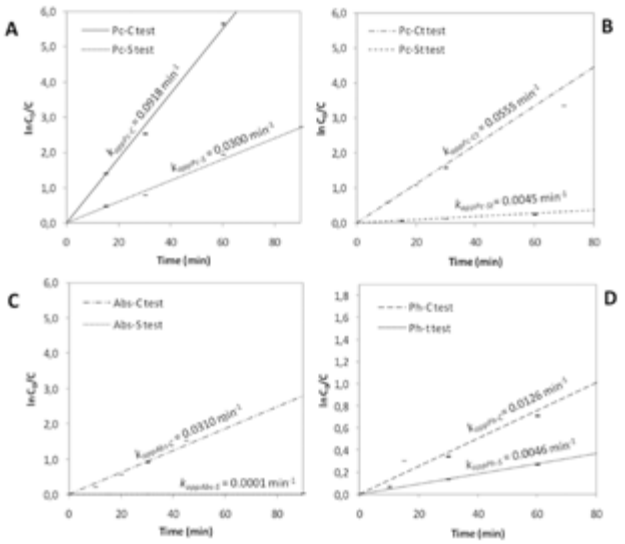

Figure 4. Linearized kinetic curves with apparent kinetic constant values (k_{app}) of CV removal. Kinetic comparison between: photocatalysis using the photoactive coating (**Pc-C** test) and TiO_2 slurry (**Pc-S** test) (A); photocatalysis in the presence of $CaSO_4$ particles using the photoactive coating (**Pc-Ct** test) and TiO_2 slurry (**Pc-St** test) (B); absorption on the photoactive coating (**Abs-C** test) and on TiO_2 slurry (**Abs-S** test) (C); photolysis in the presence of $CaSO_4$ particles (**Ph-t** test); photolysis with the photoactive coating in the presence of the barrier coating (**Ph-C** test) (D).

enabled the comparison of the apparent rate constants (k_{app}). The comparison between the linearized kinetic curves of CV photodegradation reactions obtained during **Pc-C** and **Pc-S** tests as well as **Pc-Ct** and **Pc-St** tests is reported in Figures 4-A and 4B, respectively. Linearized kinetic curves of CV absorption by **Abs-C** and **Abs-S** tests as well as CV photolysis by **Ph-t** and **PhC** tests are compared in Figures 4-C and 4-D

Test	Description (*catalyst*)	k_{app} (min^{-1})	deg_{60} (%)
Pc-C	Photocatalysis (*photoactive coating*)	0.0918	99
Pc-Ct	Photocatalysis in turbid conditions[a] (*photoactive coating*)	0.0555	97
Pc-S	Photocatalysis in slurry (*TiO_2 powder*)	0.0300	86
Pc-St	Photocatalysis in slurry and turbid conditions[a] (*TiO_2 powder*)	0.0045	23
Ph-C	Photolysis (*barrier coating on photoactive coating*)	0.0126	51
Ph-t	Photolysis in turbid conditions[a]	0.0046	24
Abs-C	Absorption (*photoactive coating*)	0.0310	88
Abs-S	Absorption in slurry (*TiO_2 powder*)	0.0001	3

a. Turbid conditions were obtained by dispersing $CaSO_4$ powder (8 g/L) in the aqueous CV solution.

Table 2. CV degradation calculated apparent kinetic constants and percent degradation after 60 min treatment.

The photoactive coating achieved a photoabatement rate with a $k_{appPc\text{-}C}$ of 0.0918 min^{-1}: this value resulted more than three times higher than $k_{appPc\text{-}S}$ ($k_{appPc\text{-}S}$ = 0.0300 min^{-1}) obtained in **Pc-S** test (Figure 4-A). Once again, in the **Pc-C** test, the pollutant removal was completed after 60 min (see Table 2). Moreover, at low CV concentration, the TiO_2- embedded photoactive coating exhibited evident higher photoactivity than dispersed TiO_2. Working with TiO_2 slurry as a catalytic system (**Pc-S** test), the observed CV degradation was 86% after 60 min, corresponding to a photoabatement rate, $k_{appPc\text{-}S}$, of 0.0300 min^{-1}. The complete degradation of CV by means of the TiO_2 dispersion was achieved after 120 min.

The presence of $CaSO_4$ particles (8 g/L) partially lowered the photocatalytic activity of the TiO_2-embedded photoactive coating. In fact, in the **Pc-Ct** test (Figure 4-B), the observed photoabatement rate, $k_{appPc\text{-}Ct}$, was equal to 0.0555 min^{1} and a CV abatement of 97% was reached after 60 min (Table 2). The $k_{appPc\text{-}Ct}$ value was lower than $k_{appPc\text{-}C}$ because in highly turbid conditions the photolysis contribution to CV degradation was strongly diminished. The photocatalytic coating at the end of **Pc-C** and **Pc-Ct** tests turned in a transparent-white hue revealed that the absorbed CV was completely decomposed by the photoactive coating in both clear and turbid conditions. These results are in agreement with the deg_{60} *(%)* value obtained during **Pc-C** and **Pc-Ct** tests: 98.7% and 96.6%, respectively. In **Ph-t** and **Pc-St** tests (Figures 4-B and 4-D), the dye degradation rates, $k_{appPh\text{-}t}$ and $k_{appPc\text{-}St}$, resulted reduced to the values 0.0046 min^{-1} and 0.0045 min^{1}, respectively (Table 2), because of the UV blocking effect of turbidity due to dispersion of $CaSO_4$ particles (8 g/L).

Absorption (**Abs-C**, **Abs-S**) and photolysis (**Ph-C**, **Ph-t**) tests were also performed (Figures 4-C and 4-D). The decrease in CV concentration observed during absorption tests could be described as a simple mass transfer of the pollutant from the aqueous phase to the photocatalytic coating (**Abs-C**) or onto TiO_2 slurry particles (**Abs-S**). In particular, in the **Abs-C** test, CV molecules were chemically unaltered and underwent to a simple phase-transfer from the solution into the photoactive coating. Thus, at the end of the test the photoactive coating exhibited a bright hue due to the presence of the triarylmethane dye.

The photolysis test in the presence of the barrier coating (**Ph-C**) was specifically set in order to evaluate the mere photolytic effect of UV light towards CV and to exclude absorption into the ionomeric coating (Figure 4-D). The calculated $k_{appPh\text{-}C}$ value ($k_{appPh\text{-}C}$ = 0.0126 min^{-1}) revealed that CV is slightly more sensitive towards UV radiations than other basic dyes, such as RhB (5). Moreover, the comparison of the calculated kinetic parameters presented in Table 2 allowed us to assess that the dye absorption onto the catalyst slurry particles ($k_{appAbs\text{-}S}$ = 0.0001 min^{-1}) was evidently negligible if compared to the corresponding photodegradation rate ($k_{appPc\text{-}S}$ = 0.0300 min^{-1}). Quantum yield (QY) and quantum efficiency (QE) of the abatement process were estimated through Equations 2 and 3 (30):

$$QY = \frac{k_{app}[CV]_0 V}{\Phi_{Abs}} \quad \text{(Eq.2)} \qquad QE = \frac{k_{app}[CV]_0 V}{\Phi_{IN}} \quad \text{(Eq. 3)}$$

where k_{app} is the calculated apparent kinetic constant expressed in s^{-1}, $(CV)_0$ the initial concentration of CV, *V* the volume of the solution, Φ_{Abs} the absorbed fraction of molar photon flux expressed in $mol \cdot s^{-1}$ and Φ_{IN} the average molar photon flux guaranteed by the UV lamp. In particularly, QY and QE were evaluated for the photoactive coating (**Pc-C** test) and compared to the performances obtained with TiO_2 slurry (**Pc-S** test): in the **Pc-C** test, QY and QE were 89% and 48%, respectively; in the **Pc-S** test they resulted 29% and 16%, respectively. The comparison of QY and QE values showed definitely higher yield and efficiency of the photoactive coating compared to the TiO_2 slurry. In particular, the light absorption due to the TiO_2 within the photoactive coating ($66 \cdot 10^{-3}$ W/m^2) resulted similar to that due to the TiO_2 slurry ($55 \cdot 10^{-3}$ W/m^2).

Thus, the comparison of QY and QE values showed definitely higher yield and efficiency of the photoactive coating compared to the TiO_2 slurry. On the basis of these results, a further optimization of the performances of photoactive coating can be fruitfully obtained by increasing its thickness.

CONCLUSIONS

An evident and useful synergic effect between TiO_2 and perfluorinated ionomeric materials was proven in the photocatalytic abatement of CV, as specific dye. Indeed, an AQ/AD-based coating with embedded TiO_2 was developed and it resulted considerably more efficient than TiO_2 slurry in water remediation of CV-polluted aqueous solutions in both transparent and turbid conditions. In addition, the photoactive fluorinated coating conveniently avoided the separation of catalyst from purified water. Overall, this photocatalytic system can remain active in case of slime deposition on the photoactive surface and, therefore, it emerges as suitable technology for the development of continuous industrial plants. Investigations on visible light activated TiO_2 and photoinduced purification of gas-phase pollutants are future studies for this promising TiO_2-based photoactive coating.

ACKNOWLEDGMENTS

The authors wish to acknowledge the generous support and the valuable interactions induced to this research in the field of fluorinated materials by the institution of the Politecnico di Milano/Solvay Fluorine Chemistry Chair. This work has been supported by MIUR (PRIN 2010-2011, prot. 2010PFLRJR).

REFERENCES

1. C. Galindo, P. Jacques, A. Kalt, Chemosphere 45 (2001) 997-1005.
2. G. Mele, G. Ciccarella, G. Vasapollo et al., B 38 (2002) 309-319.
3. M. Sansotera, F. Persico, C. Pirola, et al., B 148 (2014) 29-35.
4. A. Polo, M. V. Diamanti, T. Bjarnsholt, et al., Photochem. Photobiol. 87 (2011) 1387-1394.
5. F. Persico, M. Sansotera, C. L. Bianchi, et al. 170 (2015) 83-89.
6. M. Sansotera, F. Persico, V. Rizzi, et al, Fluorine Chem. 179 (2015) 159-168.
7. A. Fujishima, T. N. Rao, D. A.Tryket al., C 1 (2000) 1-21.
8. K. Sato, T. Hirakawa, A. Komano, et al., B 106 (2011) 316-322.
9. S. R. Seagle, in: J. I. Kroschwitz (Ed.) The Kirk Othmer Encyclopedia of Chemical Technology, fourth ed., John Wiley and Sons, New York, 1997, Vol. 24, pp. 186-224.
10. M. A. Henderson, Surf. Sci. Rep. 66 (2011) 185-297.
11. J. Sun, X. Yan, K. Lv, et al. A: Chem. 367 (2013) 31-37.
12. F. Persico, M. Sansotera, M. V. Diamanti, et al., Thin Solid Films 545 (2013) 210-216.
13. A. Mills, S. Le Hunte, J. Photochem. Photobiol., A 108 (1997) 1-35.
14. C. L. Bianchi, S. Ardizzone, G. Cappelletti, et al. Res. 25 (2010) 96-103.
15. W. Navarrini, T. Brivio, D. Capobianco, et al. Technol. Res. 8 (2011) 153-160.
16. D. M. Lemal, J. Org. Chem. 69 (2004) 1-11.
17. C. Corvaja, G. Farnia, G. Formenton, et al. Chem. 98 (1994) 2307-2313.
18. M. Yamabe, H. Miyake, in: R. E. Banks, B. E. Smart, J. C. Tatlow (Eds.), Organofluorine Chemistry, Plenum Press, New York/London, 1994, pp. 397-410.
19. W. Navarrini, M. V. Diamanti, M. Sansotera, et al. Prog. Org. Coat. 74 (2012) 794-800.
20. M. Avataneo, W. Navarrini, U. De Patto, et al. Chem. 130 (2009) 933-937.
21. M. Sansotera, W. Navarrini, M. Gola, et al. Fluorine Chem. 132 (2011) 1254-1261.
22. H. Zhang, P. K. Shen, Chem. Rev. (Washington, DC, U. S.) 112 (2012) 2780-2832.
23. W. G. Grot, Fluorinated Ionomers, W. Andrew (Ed.), PDL Handbook Series, Elsevier, Amsterdam, 2008, pp. 75-135.
24. J. R. O'Dea, N. J. Economou, S. K. Buratto, Macromolecules 46 (2013) 2267-2274.
25. W.-L. W. Lee, S.-T. Huang, J.-L. Chang, et al. Catal. A: Chem. 361-362 (2012) 80-90.
26. H.-J. Fan, C.-S. Lu, W.-L. W. Lee, et al. Hazard. Mater. 185 (2011) 227-235.
27. T. Stanoeva, D. Neshchadin, G. Gescheidt, et al. Chem. A 109 (2005) 11103-11109.
28. E. Q. Adams, L. Rosenstein, J. Amer. Chem. Soc. 36 (1914) 1452-1473.
29. W. Navarrini, B. Scrosati, S. Panero, et al. Sources 178 (2008) 783-788.
30. N. Serpone, J. Photochem. Photobiol., A 104 (1997) 1-12.

FOSSIL RESOURCES ARE IN MANY OF OUR DAY TO DAY PRODUCTS... EVEN THINGS WE DON'T REALIZE

CARBON CAN BE NEW

OR CARBON CAN BE RECYCLED

WHERE THIS CARBON COMES FROM IS UP TO YOU

LanzaTech

RECYCLED CARBON TODAY FOR A CLEANER TOMORROW

LanzaTech

CHOOSE RECYCLED CARBON: IT JUST MAKES SENSE

WWW.LANZATECH.COM